Scientific Research Publishing

Food and Nutrition Sciences, 2023, 14, 601-625
https://www.scirp.org/journal/fns
ISSN Online: 2157-9458
ISSN Print: 2157-944X

Development of Active Films with Collagen Fiber and Polyvinyl Alcohol Mixture and Incorporation of Oregano and Rosemary Essential Oils in Their Matrix

Suslin Raatz Thiel[1*], Mari Silvia Rodrigues De Oliveira[1], Vinícius Badia[2], Stephanie Reis Ribeiro[1], Roger Wagner[1], Tatiana Emanuelli[1], Rosa Cristina Prestes[1#], Renius Mello[1]

[1]Department of Food Science and Technology, Federal University of Santa Maria, Santa Maria, Brazil
[2]Department of Food Engineering and Chemical Engineering, Santa Catarina State University, Pinhalzinho, Brazil
Email: *suslin.thiel@gmail.com

How to cite this paper: Thiel, S.R., De Oliveira, M.S.R., Badia, V., Ribeiro, S.R., Wagner, R., Emanuelli, T., Prestes, R.C. and Mello, R. (2023) Paper Title. *Food and Nutrition Sciences*, **14**, 601-625.
https://doi.org/10.4236/fns.2023.147040

Received: June 3, 2023
Accepted: July 21, 2023
Published: July 24, 2023

Abstract

The aim was to develop films with a new mixture of collagen fiber plus polyvinyl alcohol added of oregano or rosemary essential oils at different levels (0%, 2%, 4% and 6%), as well as to assess the antimicrobial activity, physical, optical, microstructure and molecular properties in the films. An interaction between the ingredients was observed at the molecular level by FTIR. The amide II and amide III bands, which are important to verify collagen conformation, showed intense peaks in the films. The formation of a network through collagen fibers was produced, acting as a reinforcement in matrix. The films with essential oil had an expressive antimicrobial activity by the steam contact method (micro-atmosphere), mainly for *Escherichia coli* and *Staphylococcus aureus*. The mixture of collagen fiber plus polyvinyl alcohol added of essential oils is a promising matrix for application in food as active packaging.

Keywords

Antimicrobial Activity, Biodegradable Packaging, Bioactive Volatile Compounds, Fourier Transformed Infrared Spectroscopy, Scanning Electron Microscopy, Sustainable Packaging

1. Introduction

Packaging plays a key role in protecting, facilitating handling, and promoting

*Corresponding author.
#In memorium.

communication with consumers. Nevertheless, the functionality of packaging has increased over time, and it no longer has only its basic functions [1]. Active packaging is a new concept because of its ability to interact with the internal environment; it can extend the shelf life of these products, reducing waste by incorporating bioactive compounds into the matrix of the films/packaging that has biological activities [1] [2] [3]. Incorporating bioactive compounds into foods, such as essential oils and extracts, has been studied by numerous researchers. However, depending on the concentrations used, they can alter the product's sensory characteristics, decreasing consumers' acceptance and making adding these compounds to films/packaging an interesting topic [4].

Essential oils and their antimicrobial and antioxidant activities are well-known in the food industry [3]. The *Lamiaceae* family is widely studied for its bioactive compounds, including oregano (*Origanum vulgare*) and rosemary (*Rosmarinus officinalis*).

It is estimated that roughly 359 million tons of plastics are manufactured annually worldwide, of which biodegradables account for only 1%. Many of these materials are destined to manufacture flexible packaging [5]. Due to the environmental impact caused by the exacerbated use of synthetic materials, the food industry generates a large part of this impact through packaging. The use of raw materials obtained from renewable and abundant sources for producing films is an exciting concept from the point of view of biodegradable material production. Extracted from bovine slaughter by-products, collagen fibers (CF) of bovine origin can be extracted from the dermis and subcutaneous tissue [6]. Films produced with collagen stand out from those produced with other proteins due to their high strength characteristics, low water solubility, and fibrous microstructure [4] [7]. Biodegradable synthetic polymer polyvinyl alcohol (PVA) is water soluble, non-toxic, and can interact with other biodegradable materials due to hydrogen bond formation [8]. Despite various studies in developing flexible films for food, there is still a gap in the literature as many studies do not present the necessary characteristics for their applications.

Given the above, the aim was to evaluate the chemical composition and antimicrobial activity of oregano and rosemary essential oils; to develop films with a mixture of collagen fiber plus polyvinyl alcohol added or no of essential oils; and, to analyze *in vitro* the antimicrobial capacity, physical properties, optics, microstructure and molecular structure of the films.

2. Materials and Methods

2.1. Materials

The bovine collagen fiber was supplied by NovaProm Food Ingredients (São Paulo, SP/Brazil). The synthetic PVA was acquired from Kuraray (São Paulo, SP/Brazil). The oregano and rosemary (pre-dehydrated) were purchased locally (Chapecó, SC/Brazil). The other reagents were of analytical quality and included brain heart infusion (BHI) broth (Kasvi, Spain), BHI Agar (Kasvi, Spain), tryp-

tone soy broth (TSB) (Kasvi, Spain), sodium chloride (Synth, Brazil), acetic acid (Vetec, Brazil), Tween 80 (InduLab, Brazil), glycerol (Dinâmica, Brazil), resazurin (Sigma Aldrich, USA), and potassium nitrate (Dinâmica, Brazil).

2.2. Methods

2.2.1. Bacteria

The strains were stored under freezing (−18˚C) in TSB and glycerol mixture until the time of use. Before the experiments, the strains were grown twice on tilted BHI agar and incubated in a microbiological oven at 37˚C for 24 h. Bacteria from the American Type Culture Collection (ATCC) were used: *Staphylococcus aureus* (SA) (ATCC 6538), *Escherichia coli* (EC) (ATCC 8739), *Pseudomonas aeruginosa* (PA) (ATCC 9027), *Salmonella* typhimurium (ST) (ATCC 1408), *Listeria monocytogenes* (LMB) (biofilm forming) (ATCC 7644), and *Listeria monocytogenes* (LMSA) (Scott A).

2.2.2. Oregano and Rosemary Essential Oil Extraction

The essential oils were extracted using the steam distillation method [9].

2.2.3. Oregano and Rosemary Essential Oil Characterization

The chemical characterization of the oregano (OEO) and rosemary (REO) essential oils was performed by gas chromatography coupled to mass spectrometry (GC/MS Shimadzu QP2010 Plus; Shimadzu Corporation, Tokyo, JP) with a ZB – 5 MS capillary column (30 m × 0.25; 0.25 mm, flow rate 1 mL/min). The ramp conditions were 40˚C for 1 min and 230˚C at a rate of 4˚C/min for 3 min and the injector at 250˚C. A series of n-alkanes was analyzed under the same chromatographic conditions to calculate the linear retention index (LRI). Identification was made by comparing with mass spectra from the National Institute of Standards and Technology (NIST) and experimental LRI with those available in the literature.

2.3. Antimicrobial Activity of the Oregano and Rosemary Essential Oil Extraction

2.3.1. Minimum Inhibitory and Bactericidal Concentrations

Minimum inhibitory concentration (MIC) analysis was based on the broth microdilution technique [10]. The essential oils (EOs) were diluted to 25% (w/v) in BHI broth supplemented with 3% Tween 80, and serial dilutions were performed in the microplate for the OEO (240 - 0.12 mg/mL) and REO (229.12 - 0.111 mg/mL). Dilutions were calculated based on the density of the EOs: 0.9618 g/mL for the OEO and 0.9165 g/mL for the REO. The concentration of the bacteria of interest was adjusted to 1.5×10^8 (0.5 McFarland) in 0.85% saline solution. Subsequently, 10 µL of the bacterial suspension was added to each well, followed by homogenizing each well of the microplate. The plates were covered and incubated in a bacteriological oven at 37˚C for 24 h. Afterward, 10 µL of resazurin solution (0.01%) was added to verify if the target bacteria was inhibited, and the color blue characterized bacterial inactivity and red characterized activity [11].

For the minimum bactericidal concentration (MBC), all concentrations that inhibited the target bacterium were used, and a 10-µL aliquot was taken and deposited in Petri plates containing BHI agar. The plates were incubated in an incubator at 37˚C for 24 h. The lowest concentration at which no microbial growth occurred on the plate was the MBC.

2.3.2. Micro-Atmosphere

The micro-atmosphere analysis was based on the method of Ghabraie *et al.* [12] with modifications. The concentration of the bacterium of interest was first adjusted (0.5 McFarland), followed by depositing 100 µL of the solution into Petri dishes containing BHI agar. After the plates dried, a sterile paper disk was inserted into the lid of the Petri dish, and a 30-µL aliquot of the EO was inserted (30 µL of sterile distilled water was used for the control plates). Immediately afterward, the plates were sealed with Parafilm®. The plates were incubated at 37˚C for 24 h. Afterward, the total inhibition halo was measured using a manual pachymeter (Messen, Brazil).

2.4. Film Preparation

The films were developed according to Paglione *et al.* [13] with modifications. A mixture of collagen fiber (5.0% w/v), polyvinyl alcohol (5.0% w/v), Tween 80 (1.0%), and glycerol (1.30%) was made. The pH of the solution was set to 3.0 using a 50% acetic acid solution. The solution was homogenized for 3 min with a homogenizer (Turratec, Tecnal, TE 102). The solutions were then heated at 90˚C for 20 min in an ultra-thermostatic bath (Solab, Model SL 152). After the heating time, 2%, 4%, and 6% concentrations of the OEO or REO were added. The control solution did not contain the addition of EO. The solutions were then placed in an ultrasound bath (Ultronique, Model Q3.8/40A) to remove the bubbles formed for 5 min at room temperature. Each solution was inverted in glass plates (29.7 × 21.0 cm) and placed in an oven with air circulation (Marconi, Model MA035) for roughly 24 h. The films were then stored until the respective analyses in desiccators with saturated potassium nitrate solution (RH 60% and 25˚C) controlled by a thermo-hygrometer (Akso-AK28).

2.5. *In Vitro* Antimicrobial Activity of the Films

2.5.1. Disk Diffusion

Aliquots of 100 µL of the bacteria of interest (0.5 McFarland) were inoculated into Petri plates containing BHI agar. The developed films were aseptically cut into 20-mm disks, positioned in the center of the plate, and incubated in an incubator at 37˚C for 24 h. After the elapsed time, only the inhibition halo was measured with a manual pachymeter (Messen, Brazil).

2.5.2. Micro-Atmosphere

The analysis was performed as described in item 2.5.1, although the 20-mm disks were deposited on the inner face of the lid of the Petri dish in this assay.

The plates were then sealed with Parafilm®. The total inhibition zone (including the film) was measured with a manual pachymeter (Messen, Brazil).

2.6. Film Characterization

2.6.1. Film Thickness

The films' thickness was measured using a manual micrometer (Messen, Brazil) by randomly reading at 10 points.

2.6.2. Optical Properties

In order to determine the L^*, a^* and b^*, C^*, h^*, and opacity values of the films, six readings were taken using a spectrophotometer (Model CM-700d, Konica Minolta Sensing Inc., Japan). The films were placed on a standard white plate (L = 88.66, a = 0.3, and b = 3.36). Readings were taken using D65 illuminant, specular component excluded (SCE), 8 mm measurement area (MAV), and a 10˚ observation angle.

The total color difference (ΔE) was calculated using Equation (1):

$$\Delta E = \left[\left(\Delta L^* \right)^2 + \left(\Delta a^* \right)^2 + \left(\Delta b^* \right)^2 \right]^{0.5} \quad (1)$$

The opacity was calculated by the overlapping ratio of the black standard (S_{black}) and white standard (S_{white}) according to Equation (2) [14]:

$$\text{Opacity} = S_{\text{black}} / S_{\text{White}} \times 100 \quad (2)$$

2.6.3. Scanning Electron Microscopy

The films' surface microstructure images were determined with an electron microscope (JEOL, model JSM-6360) with a 10 kV electron beam. The samples were dried in an air oven at 30˚C for 12 h. The film samples were adhered to the surface of double-sided carbon strips and then coated with a gold layer using a vacuum metallizer for 40 s (Denton Desk V; Denton Vacuum, USA). Surface images were taken at 100× and 1000× magnifications.

2.6.4. Fourier Transform Infrared Spectroscopy

The infrared spectrometry analyses were performed in infrared spectroscopy (Prestige, Shimadzu) by the direct transmittance method using the KBr tablet technique. The spectra were obtained in the 400 - 4500 cm^{-1} range with 45 scans and a resolution of 2.0 cm^{-1}.

2.7. Statistical Analysis

For the bacterial susceptibility (micro-atmosphere) of the pure essential oils, a completely randomized factorial experimental design with four replications arranged in a 2 × 6 factorial scheme (2 types of essential oil × 6 microorganisms) was used.

For bacterial susceptibility (diffusion disk and micro-atmosphere) of the films, a completely randomized experimental design with a 2 × 4 × 6 factorial arrangement (2 types of essential oil × 4 levels of essential oil × 6 microorganisms)

was used, totaling 48 treatments with four repetitions each, according to the statistical model:

$$Y_{ijkl} = \mu + \alpha_i + \beta_j + \gamma_k + (\alpha\beta)_{ij} + (\alpha\gamma)_{ik} + (\beta\gamma)_{jk} + (\alpha\beta\gamma)_{ijk} + \varepsilon_{ijkl} \quad (3)$$

where, Y_{ijkl} = value observed in the *i*-th essential oil type, *j*-th level of essential oil, *k*-th microorganism, and *l*-th repetition; μ = overall mean of the response variable; α_i = fixed effect of *i*-th type of essential oil; β_j = fixed effect of the *j*-th level of the essential oil; γ_k = fixed effect of the *k*-th microorganism; $(\alpha\beta)_{ij}$, $(\alpha\gamma)_{ik}$, and $(\beta\gamma)_{jk}$ are the double interactions; $(\alpha\beta\gamma)_{ijk}$ corresponds to the triple interaction; and ε_{ijk} = random effect associated with the observation Y_{ijkl}, assumption $\varepsilon_{ijkl} \overset{iid}{\sim} N(0, \sigma^2)$.

For thickness and color (L^*, a^*, b^*, C, h°, opacity, and ΔE), a completely randomized design with a 2 × 4 factorial arrangement (2 types of essential oil × 4 essential oil levels) was used, totaling 8 treatments with four repetitions each.

The data were subjected to univariate analysis of variance (ANOVA), their means were adjusted by ordinary least squares and compared by the Student Newman Keuls (SNK) test. For the essential oil levels, linear and quadratic tendency were evaluated using orthogonal contrast analysis from the coefficients for interpolation of orthogonal polynomials. Subsequently, polynomial regression analysis was performed to investigate the changes in the dependent variables as a function of the essential oil level. The values of the determination coefficient (r^2) were expressed in relation to the treatment sources (regression + lack of adjustment).

The Fourier Transform Infrared Spectroscopy (FTIR) spectral data in the 4000 - 400 cm^{-1} region were submitted to chemometric analysis. Initially, the spectra were linearized; for this, the first and second derivatives were tested. Then, the multivariate techniques of cluster analysis (CA) and principal component analysis (PCA) were used to reduce the dimensionality of the data and verify differences between treatments.

The statistical analyses were performed in R and RStudio at 5% significance level [15] [16].

3. Results and Discussion

3.1. Composition of Essential Oils

Twenty compounds were identified for the OEO (oregano essential oil): thymol (29.44%), (E)-sabinene hydrate (24.18%), p-cymene (17.94%), terpinen-4-ol (5.52%), linalool (4.91%), (Z)-sabinene hydrate (2.48%), α-terpineol (2.19%), carvacrol (1.86%), D-limonene (1.65%), sabinene (1.56%), caryophyllene oxide (1.53%), carvacrol methyl ether (1.22%), cis-p-menth-2-en-1-ol (0.98%), myrcene (0.96%), thymol methyl ether (0.72%), α-thujene (0.69%), spathulenol (0.67%), β-bisabolene (0.61%), α-pinene (0.48%), and β-pinene (0.40%). Thymol was the main compound found for OEO, corroborating Barbosa *et al.* [17]. However, some studies have reported that the main compound in OEO is carvacrol [18].

In the REO (rosemary essential oil), 28 compounds were identified: 1,8-cineole (46.63%), camphor (13.83%), *α*-pinene (13.63%), *β*-pinene (4.08%), camphene (4.08%), *β*-caryophyllene (3.90%), borneol (3.38%), *α*-terpineol (2.66%), p-cymene (1.90%), *β*-myrcene (1.40%), linalool (0.97%), terpinen-4-ol (0.80%), *γ*-terpinene (0.48%), *α*-terpinene (0.43%), *α*-humulene (0.40%), bornyl acetate (0.33%), terpinolene (0.24%), *α*-phellandrene (0.17%), tricyclene (0.12%), 1-octen-3-ol (0.11%), caryophyllene oxide (0.11%), *β*-bisabolene (0.10%), *α*-thujene (0.09%), camphene hydrate (0.05%), σ-cadinene (0.04%), dehydrosabinene (0.03%), 3-octanone (0.02%), and trans-pinocarveol (0.02%). 1,8-cineolee was the major compound in the REO, followed by camphor and *α*-pinene. Cariri *et al.* [19] also found the same major compounds.

3.2. Antimicrobial Activity of Essential Oils

The MIC (minimum inhibitory concentration) (mg/mL) and MBC (minimum bactericidal concentration) (mg/mL) of the OEO (oregano essential oil) were: 7.51 and 7.51 for *Escherichia coli* (EC), 30.05 and 30.05 for *Listeria monocytogenes* (Biofilm) (LMB), 30.05 and 60.11 for *Listeria monocytogenes* (Scot A), 15.02 and 60.11 *Pseudomonas aeruginosa* (PA), 15.02 and 30.05 *Staphylococcus aureus* (SA), and 15.02 and 30.05 *Salmonella* typhimurium (ST), respectively. In the REO, the MIC (mg/mL) and MBC (mg/mL) were 28.64 and 57.28 for EC, 229.12 and 229.12 for LMB, and 57.28 and 229.12 for ST, respectively. With the analyzed REO (rosemary essential oil) concentrations, for some bacteria, it was only possible to verify the MIC: LMSA (229.12), PA (114.56), and SA (229.12).

The bacteria were more sensitive to the OEO, and similar data were reported by Silva *et al.* [20] and Alvarez *et al.* [21]. In addition, no differences in efficacy were observed between Gram-positive and Gram-negative bacteria.

The EC showed higher sensitivity, whereas lower sensitivities were presented by LMSA and LMB for the OEO and REO compounds. The SA bacteria also showed lower sensitivity to the REO. Lower values have also been reported elsewhere for the EO of a Mexican oregano species (0.25 - 0.5 mg/mL, MIC) and 0.5 - 0.75 mg/mL, MBC), Greek oregano (0.25 - 0.5 mg/mL, MIC; 1 - 2 mg/mL, MBC), common oregano (2 - 8 mg/mL, MIC; 8 - 16 mg/mL, MBC) [18] [22]. Nevertheless, for the SA bacteria, we observed lower MIC (15.02 mg/mL) and MBC (30.05 mg/mL) values compared to Kosakowska *et al.* [18] for a common oregano species (32 mg/mL MIC and 64 mg/mL MBC). Literature data indicate chemical composition near those obtained in our analyses. The concentration of thymol (29.44%) was higher than in other studies (0.58% - 28.31%). In contrast, carvacrol (1.86%) was lower (4.64% - 37.21%). Large amounts of this compound (88.50 and 66.89%) in OEO are responsible for the high antimicrobial activity [23]. Although there is a difference in the location of the functional group in thymol and carvacrol molecules, their effects are similar [24].

Lower MIC values in Gram-negative (2.75 - 5.50 mg/mL) and Gram-positive (0.70 - 2.25 mg/mL) bacteria have already been reported for REO [23]. The

composition of REO in the literature was also close to this study, and differences were found for linalool. 1,8-Cineole was identified as one of the main ones responsible for the activity due to the changes it causes in the shape and size of Gram-positive and Gram-negative bacteria; synergistic action with the other compounds has also been suggested [25].

The micro-atmosphere analysis assesses the biological activity in the steam phase. Differences were observed when comparing the results between MIC and MBC, and such differences have also been reported elsewhere [12].

The highest ($p < 0.05$) sensitivities were shown for LMSA, SA, and ST bacteria for OEO (**Table 1**). The OEO showed higher ($p < 0.05$) inhibitions in all bacteria, while the REO showed no activity in the steam phase, albeit only for ST bacteria. Among Gram-negative bacteria, PA is less sensitive to the action of Eos [26]. Nevertheless, the REO showed one of the highest inhibition activities compared to the other bacteria analyzed. López *et al.* [27] did not find inhibitory activity in the steam phase for pure REO for any bacteria. Differences in the biological activity of EOs are expected, as their chemical composition directly influences their bioactivity [28].

3.3. *In Vitro* Antimicrobial Activity of the Films

The developed films showed activity against all pathogenic bacteria analyzed, proving that the matrix CF and PVA is promising for applying EOs. According to Seydim and Sarikus [29], in addition to the composition of the EO present in the film matrix, the material used in the film is fundamental to promoting biological activity through the release property of the EO constituents.

Table 1. Bacterial susceptibility in micro-atmosphere (mm) to rosemary (*Rosmarinus officinalis* L.) and oregano (*Origanum vulgare* L.) essential oils.

Bacteria[1] (B)	Essential oil (EO)		Mean	*p*-value	
	Oregano	Rosemary		Source	Pr > F
EC	35.8^{Ba}	16.3^{Bb}	26.0	EO	0.0001
LMB	32.0^{Da}	19.5^{Ab}	25.7	B	0.0001
LMSA	39.7^{Aa}	16.8^{Bb}	28.3	EO × B	0.0001
PA	34.5^{Ca}	19.0^{Ab}	26.7		
SA	40.6^{Aa}	11.5^{Cb}	26.0		
ST	39.5^{Aa}	0.0^{Db}	19.7		
Mean	37.0	13.8		SEM[2] = 1.9	CV[3] = 3.1

Means followed by different capital letters within the same column and different small letters within the same row differ ($p < 0.05$), respectively, between bacteria and essential oil by the Student Newman Keuls test. [1]EC = *Escherichia coli*; LMB = *Listeria monocytogenes* (biofilm); LMSA = *Listeria monocytogenes* (Scott A); PA = *Pseudomonas aeruginosa*; SA = *Staphylococcus aureus*; ST = *Salmonella* typhimurium. [2]SEM = Standard error of the mean. [3]CV = Coefficient of variation.

Levels of EO were incorporated into the CF plus PVA film, and their inhibition potential was verified by the disk-diffusion method. The control films (without adding the EO) showed no inhibitory effect for all bacteria. The regression equations for each bacterium as a function of OEO or REO concentration showed different behaviors for the disk-diffusion analysis (**Figure 1(A)** and **Figure 1(B)**). Higher OEO concentrations were necessary to inhibit LMSA, EC, and SA compared to REO. However, the point of maximum inhibition was higher for OEO.

In the OEO, the equations for LMSA, LMB, PA, and ST bacteria fitted linear regression, with LMB, PA, and ST bacteria initiating their inhibitions at lower OEO concentrations. The point of maximum inhibition presented by the OEO for LMSA was similar for EC. Quadratic behavior was observed for EC and SA with the increment of OEO. Liu *et al.* [30] also found disk-diffusion inhibitions of Gram-positive and Gram-negative bacteria for soybean polysaccharide films added with OEO.

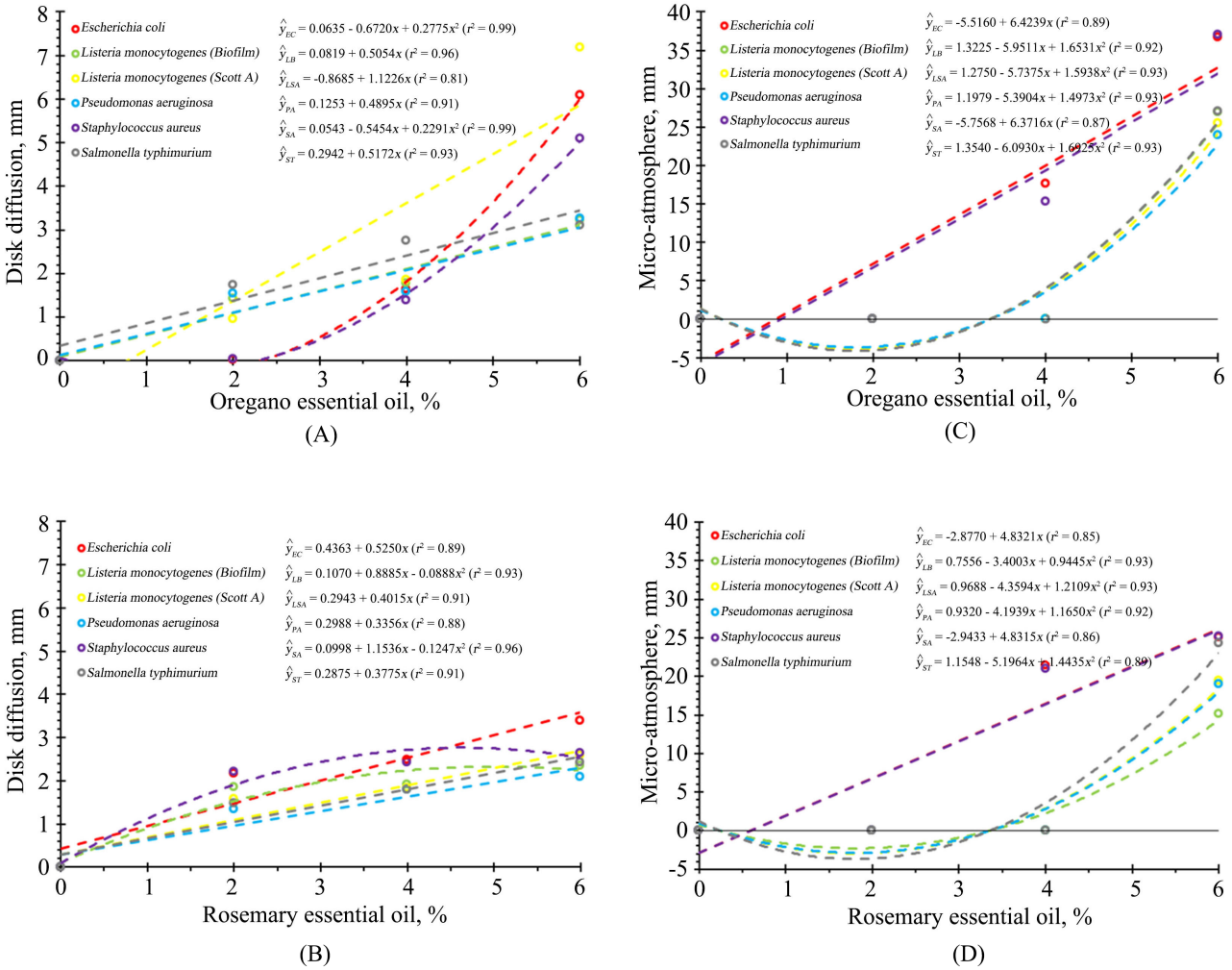

Figure 1. Bacterial susceptibility in disk diffusion (AB) and micro-atmosphere (CD) from collagen fiber plus polyvinyl alcohol films with oregano (*Origanum vulgare* L.) (AC) or rosemary (*Rosmarinus officinalis* L.) (BD) essential oil levels.

In the REO, all bacteria analyzed started their inhibitions at lower concentrations. The SA and LMB bacteria showed maximum inhibition points at 4.6% and 5.0% REO, respectively. Sani *et al.* [31] reported that protein isolate and cellulose films added with REO were more effective against Gram-positive bacteria, while chitosan films with REO showed inhibition for both Gram-positive and Gram-negative bacteria [32].

The antimicrobial activity of the films was also verified by micro-atmosphere analysis (**Figure 1(C)** and **Figure 1(D)**). We observed that higher concentrations were necessary for inhibition in the steam phase for some bacteria due to the need for volatilization of the compounds in the film matrix; thus, the volatilization properties of the EOs are important. The onset of inhibition for LMB, LMSA, PA, and ST bacteria was from the 3.5% concentration of OEO. The EC and SA showed greater sensitivity because they already had inhibition at 1% OEO. Nedorostova *et al.* [33] found that the same bacteria showed higher sensitivities in the steam phase. Hyun *et al.* [34] observed activity in the steam phase of OEO for a broad spectrum of pathogenic bacteria.

Similar behavior was noted for the REO in the micro-atmosphere; EC and SA bacteria also showed higher sensitivities (<1%). The bacteria LMB, LMSA, and PA started inhibition at 3.4% and ST at 3.5% REO. Nonetheless, OEO showed greater inhibitions with its increment.

Differences in results between the direct contact and vapor phase method have also been reported in the literature. The inhibition by direct contact is mainly linked to the more hydrophilic compounds in the EO. In the steam phase, there is a balance between hydrophilic and hydrophobic compounds [35].

As essential oil levels rise there is a higher concentration of phenolic compounds. Then, it is concluded that the biological activity of the films would be greater. Although, different behaviors were observed for some bacteria as essential oil levels raised, because they not showed difference in inhibition according to regression equations. Depending of analysis method (disk-diffusion or micro-atmosphere) and essential oil compounds, the higher amount may not affect the activity.

No higher or lower susceptibility relationship between Gram-positive and Gram-negative was observed, and differences in antimicrobial activity within the positive and negative groups were found. The EOs analyzed have a broad spectrum of activity; researchers have found that Gram-negative bacteria are less susceptible to EOs due to their outer membrane surrounding much of the cell wall [26], which was not proven in this study. However, relatively small hydrophilic or hydrophobic molecules can cross the outer membrane and access the periplasm through some proteins present, called porins [36]. Compounds such as carvacrol affect the outer membrane of Gram-negative bacteria [37]. The antimicrobial activity of REO, nevertheless, is due to the presence of phenolic compounds such as 1,8-cineole, α-pinene, and camphor with lipophilic and hydrophilic functional groups, because such compounds can interact with bacterial

cell components, disrupting the cytoplasmic membrane and affecting cell wall permeability [31].

3.4. Physical and Optical Properties of Films

The appearance of the packaging plays a determining role in the purchase of a product, in addition to the suitability for its application. The thicknesses found in CF and PVA films, plus the addition of OEO and REO, ranged from 0.22 to 0.32 mm (**Table 2**). Thickness increased ($p < 0.05$) with the addition of EO but had no effect ($p > 0.05$) on EO type. Chen *et al.* [38] found this in PVA films with EO lower thicknesses, although the higher thickness shown by the films in this study may be attributed to the joint addition of FC to PVA, generating an increase in solids in the films [39]. Chen *et al.* [38] also found slightly higher values with the addition of EO.

The color indices L^*, a^* and b^*, C value, hue angle, opacity, and color difference presented alterations. There was an effect ($p < 0.05$) of the interaction between type and level of EO on all the color attributes of the films. The films showed a tendency towards yellow (b^*) and green ($-a^*$), which can be explained by the color of the OEOs and the addition of Tween 80 [40]. With the increase of OEO, the films showed higher b^* (yellow) values ($p < 0.05$), whereas the addition of REO changed b^* values only in relation to the control (**Table 2**).

The opacity property increased ($p < 0.05$) with the increasing addition of OEO and REO. The inclusion of 6% REO provided a higher ($p < 0.05$) opacity value. Other researchers have reported similar findings [38] [41]. The higher opacity can be explained by the EO droplets causing light scattering in the film matrix [40]. However, the film matrix itself has relevance, as the control CF + PVA film also showed high values compared to other matrices. Comparing the two EOs, the REO showed higher values ($p < 0.05$) than the OEO. This increase is interesting for enhancing the film's barrier properties by blocking the passage of light [40]. Despite the high values found for opacity, the developed films presented transparency.

The addition of the EOs in the matrix of the CF + PVA film did not harm its gloss (L^*), and an increase ($p < 0.05$) in this parameter was obtained with the OEO. Interactions between the type and level of EO and the level were also observed. Shen *et al.* [40] found no significant differences with increasing OEO in starch films, and Chen *et al.* [38] reported lower L^* values in PVA films with the addition of a clove (*Syzygium aromaticum*) EO.

3.5. Scanning Electron Microscopy

The surface images of the films were used to acquire important data on the microstructure of the matrix presented with the mixture of CF (collagen fiber) and PVA (polynivyl alcohol) with the addition of the OEO (oregano essential oil) and REO (rosemary essential oil). The combination of FC and PVA (**Figure 2(A)**) showed a partially homogeneous and smooth surface structure. Interconnected fibers were observed, forming a network in which pH 3.0 has great

Table 2. Thickness and color traits from collagen fiber plus polyvinyl alcohol films with oregano (*Origanum vulgare* L.) or rosemary (*Rosmarinus officinalis* L.) essential oil levels.

Essential oil type (T)	Essential oil level (L), %				Mean
	0	2	4	6	
			Thickness, mm		
Oregano	0.22	0.31	0.31	0.32	0.29
Rosemary	0.22	0.27	0.29	0.31	0.27
Mean[1]	0.22^{b}	0.29^{a}	0.30^{a}	0.31^{a}	
			L^*		
Oregano	84.2^{Bc}	85.1^{Bab}	85.5^{Ba}	84.8^{Bb}	84.9
Rosemary	87.0^{Ab}	87.3^{Aab}	87.5^{Aa}	87.6^{Aa}	87.3
Mean	85.6	86.2	86.5	86.2	
			a^*		
Oregano	-0.31^{Ba}	-1.00^{d}	-0.84^{c}	-0.39^{Bb}	−0.63
Rosemary	-0.83^{Aa}	-0.97^{bc}	-0.90^{ab}	-0.99^{Ac}	−0.92
Mean	−0.57	−0.98	−0.87	−0.69	
			b^*		
Oregano	6.3^{Bd}	10.1^{c}	11.3^{Ab}	16.1^{Aa}	11.0
Rosemary	9.3^{Ab}	10.3^{a}	10.1^{Ba}	10.2^{Ba}	10.0
Mean	7.8	10.2	10.7	13.1	
			Chroma		
Oregano	6.4^{Bd}	10.1^{c}	11.3^{Ab}	16.2^{Aa}	11.0
Rosemary	9.4^{Ab}	10.2^{a}	10.4^{Ba}	10.7^{Ba}	10.2
Mean	7.9	10.2	10.8	13.5	
			Hue angle		
Oregano	92.4^{Bc}	95.4^{a}	94.2^{Bb}	91.1^{Bd}	93.3
Rosemary	95.5^{A}	95.4	95.7^{A}	95.8^{A}	95.6
Mean	93.9	95.4	94.9	93.4	
			Opacity		
Oregano	42.3^{Bd}	50.8^{Bc}	52.3^{Bb}	62.3^{Ba}	51.9
Rosemary	62.5^{Ad}	64.5^{Ac}	65.7^{Ab}	68.3^{Aa}	65.3
Mean	52.4	57.7	59.0	65.3	
			ΔE		
Oregano	5.23^{Bd}	7.55^{c}	8.86^{Ab}	13.56^{Aa}	8.80
Rosemary	6.87^{Ab}	7.29^{b}	7.56^{Bab}	8.14^{Ba}	7.46
Mean	6.05	7.42	8.21	10.85	

Means followed by different capital letters within the same column and different small letters within the same row differ ($p < 0.05$), respectively, between types and levels of essential oil by the Student Newman Keuls test.

[1] $\hat{y}_{Overall} = 0.2235 + 0.0353x - 0.0035x^2 \left(r^2 = 0.95\right)$.

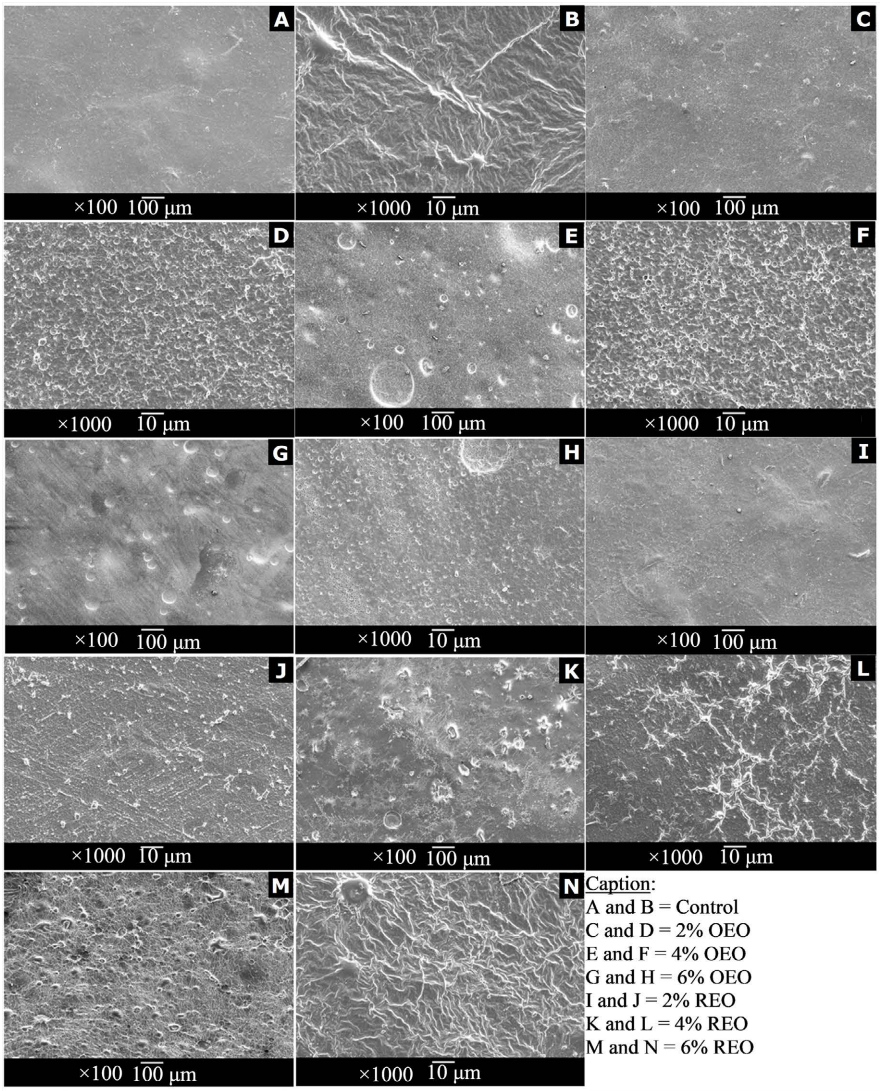

Figure 2. Surface-scanning electron microscopy (SEM) images at 100× and 1000× magnification or 100 and 10 µm resolution from collagen fiber plus polyvinyl alcohol films without (control) (AB) and with oregano (*Origanum vulgare* L., OEO) (C)-(H) or rosemary (*Rosmarinus officinalis* L., REO) (I)-(N) essential oil levels (2%, 4%, and 6%).

relevance due to the fiber's degree of intumescence, which is higher at this pH; Xu *et al.* [42] also reported a similar result. The formation of the network is also explained due to the denaturation of a part of the proteins, where there is an interaction between different bonds, such as hydrogen bonds, electrostatic and hydrophobic interactions [43]. Some protruding regions can be observed in **Figure 2(B)**, in which PVA particles were not fully solubilized in the matrix. This condition may be related to the inhomogeneity in temperature and agitation during the heating of the filmogenic solution. Films with the inclusion of the OEO showed spherical droplets on the surface. The addition of 2% OEO led to greater irregularities, as shown in **Figure 2(C)**. However, with magnification (**Figure 2(D)**), one can observe the OEO droplets distributed in the film matrix together with CF + PVA. Paglione *et al.* [13] found similar irregularities and at-

tributed them to the addition of OEO. With the increase in OEO addition (**Figure 2(E)** and **Figure 2(G)**) in the images at 100× magnification, it is possible to visualize an increase in the size of the EO droplets. At the highest OEO concentration, there was a greater distribution in the film matrix.

The REO-added films showed different structures, and the EO type, hydrophobicity, and size stability have been reported to affect the film matrix [44]. The OEO and REO showed different chemical compositions, and these differences may affect the oils' solubility in different matrices. The addition of 2% REO (**Figure 2(I)** and **Figure 2(J)**) showed no changes. With increasing REO (6%), the film showed a rough and discontinuous surface. Unlike the films that added OEO, it was impossible to visualize the REO droplets, which can be attributed to a higher interaction of REO to the matrix.

3.6. Fourier Transform Infrared Spectroscopy

The CF (collagen fiber) and PVA (polynivyl alcohol) films showed the typical bands characteristic of CF and PVA (**Figure 3**). Some changes in the position of the bands were seen with the blending for the production of the CF + PVA films and with the addition of the OEO (oregano essential oil) and REO (rosemary essential oil). The amide A band represents N-H stretching vibration [7]. This was shifted at lower frequencies for the control film (3437.30), F (Film) + 2% OEO (3420.90), F + 4% OEO (3420.90), F + 6% OEO (3427.65), F + 2% REO (3437.30), F + 4% REO (3431.41), and F + 6% REO (3421.87) cm^{-1} compared to CF (3445.98 cm^{-1}).

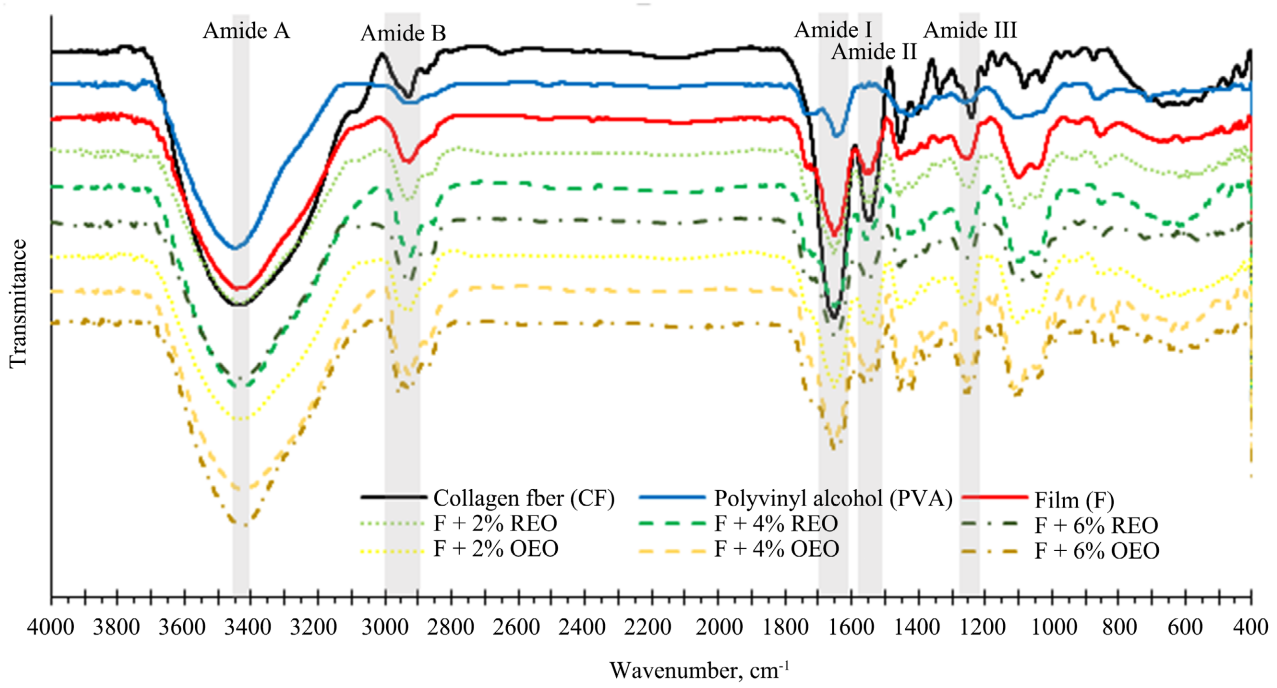

Figure 3. Fourier-transform infrared (FTIR) spectrum (4000 to 400 cm^{-1}) from collagen fiber (CF), polyvinyl alcohol (PVA), CF plus PVA film (F), and F with oregano (*Origanum vulgare* L., OEO) or rosemary (*Rosmarinus officinalis* L., REO) essential oil levels (2%, 4%, and 6%).

The PVA also showed a peak at 3447.91, which is related to the OH group [45]. The decrease is related to hydrogen bonds formed with the mixing of the materials [7] [41]. Hydrogen bonds are also involved in the process of network formation, which occurs due to partial denaturation [43]. Amide B is associated with the stretching of CH_2 [7]. We also observed the formation of new bands, and in films with OEO and REO, similar findings were found by Saricaoglu [41]. The amide I (~1700 - 1600 cm^{-1}) is sensitive to the secondary structure of the protein and is mainly known for the stretching vibration = CO [7] [45]. For CF + PVA films, lower values were found (1652.10 - 1642.46 cm^{-1}) compared to CF (1655.00 cm^{-1}). There were some changes in the conformation of collagen molecules due to the temperature used; similar data were reported by Xu *et al.* [7]. For amide II (~1600 - 1500 cm^{-1}), CF + PVA films also shifted to a higher frequency (1559.51 - 1555.66 cm^{-1}) compared to CF (1546.01 cm^{-1}); this band is characterized by C-N stretching and NH bending vibration [46].

The amide III band is mainly assigned to CN stretching, NH bending vibrations, CC stretching, and CH bending. This band is also sensitive to the secondary structure of the protein and can provide meaningful answers regarding the structural conformation of collagen [46]. For the CF + PVA films, this band was shifted to higher values compared to CF (1241.25 cm^{-1}). For the control film (1256.68), F + 2% OEO (1257.64), F + 4% OEO (1256.68), F + 6% OEO (1256.68), F + 2% REO (1248.96), F + 4% REO (1254.75), and F + 6% REO (1258.61) cm^{-1}. These results show that despite the temperature used in the manufacture of the films (90˚C/20 min), there were no major modifications of the collagen fiber structure, and a part of the fibers was not denatured (**Figure 2**).

Peaks referring to the same major compounds that were identified by GC/MS were found in the OEO- and REO-added films. Bands between 1500 - 1400 cm^{-1} are attributed to the C = C stretching vibration of the aromatic ring and bending vibration of the isopropyl methyl group in the band 1381 cm^{-1} for the p-cymene compound; for carvacrol and thymol, bands range from 1600 to 1585 cm^{-1} [47]. A band at 1591.34 cm^{-1} was only found in CF + PVA films for all added levels of OEO. The band at approximately 862 cm^{-1} strongly influences OEO [48]. In CF + PVA films with 2%, 4%, and 6% OEO, bands of 854.50, 861.25, and 863.18 were found, respectively. As for the REO-added films, bands attributed to the compound p-cymene were also identified.

4. Conclusions

The mixture of collagen fiber plus polyvinyl alcohol is interesting for film production. Collagen fiber can be extracted of residues, by- and co-products from meat industry. The use of meat processing wastes has a potential to recycle raw materials, reduce disposal, and may reduce the cost of packaging.

The incorporation of 4% essential oil into film matrix, regardless of the oil type, is the most indicated concentration to inhibit the growth of studied bacte-

ria. Nevertheless, if there is a need for inhibition a target bacterium, lower concentrations also are effective.

The *Escherichia coli* and *Staphylococcus aureus* bacteria showed greater sensitivity to the films in the vapor phase, the application as active packaging is interesting for these two strains. However, when packaging a complex matrix such as food, the added essential oil levels must be studied.

The films developed have the potential to be used as biodegradable active packaging, through protection against food pathogens and avoiding food waste.

Larger studies can be carried out to decrease the percentage of raw materials, further reducing the cost of the film.

Acknowledgements

We thank to Nathalia Daudt from the Electronic Microscopy Laboratory at UFSM for help in SEM analysis. We thank to employees at DTCA/UFSM for help during this study. The authors thank the partial funding from Coordenação de Aperfeiçoamento de Pessoal de Nível Superior (CAPES, Brasília, DF, Brazil).

Conflicts of Interest

The authors report no conflicts of interest.

References

[1] Bhargava, N., Sharanagat, V.S., Mor, R.S. and Kumar, K. (2020) Active and Intelligent Biodegradable Packaging Films Using Food and Food Waste-Derived Bioactive Compounds: A Review. *Trends in Food Science & Technology*, **105**, 385-401. https://doi.org/10.1016/j.tifs.2020.09.015

[2] Tonyali, B., McDaniel, A., Amamcharla, J., Trinetta, V. and Yucel, U. (2020) Release Kinetics of Cinnamaldehyde, Eugenol, and Thymol from Sustainable and Biodegradable Active Packaging Films. *Food Packaging and Shelf Life*, **24**, Article ID: 100484. https://doi.org/10.1016/j.fpsl.2020.100484

[3] Sharma, S., Barkauskaite, S., Jaiswal, A.K. and Jaiswal, S. (2021) Essential Oils as Additives in Active Food Packaging. *Food Chemistry*, **343**, Article ID: 128403. https://doi.org/10.1016/j.foodchem.2020.128403

[4] Asgher, M., Qamar, S.A., Bilal, M. and Iqbal, H.M.N. (2020) Bio-Based Active Food Packaging Materials: Sustainable Alternative to Conventional Petrochemical-Based Packaging Materials. *Food Research International*, **137**, Article ID: 109625. https://doi.org/10.1016/j.foodres.2020.109625

[5] European Bioplastics (2021) Bioplastics Market Data. https://www.european-bioplastics.org/market

[6] Wolf, K.L., Sobral, P.J.A. and Telis, V.R.N. (2009) Physicochemical Characterization of Collagen Fibers and Collagen Powder for Self-Composite Film Production. *Food Hydrocolloids*, **23**, 1886-1894. https://doi.org/10.1016/j.foodhyd.2009.01.013

[7] Xu, J., Liu, F., Goff, H.D. and Zhong, F. (2020) Effect of Pre-Treatment Temperatures on the Film-Forming Properties of Collagen Fiber Dispersions. *Food Hydrocolloids*, **107**, Article ID: 105326. https://doi.org/10.1016/j.foodhyd.2019.105326

[8] Bhat, V.G., Narasagoudr, S.S., Masti, S.P., Chougale, R.B. and Shanbhag, Y. (2021)

Hydroxy Citric Acid Cross-Linked Chitosan/Guar Gum/Poly(vinyl alcohol) Active Films for Food Packaging Applications. *International Journal of Biological Macromolecules*, **177**, 166-175. https://doi.org/10.1016/j.ijbiomac.2021.02.109

[9] Chemat, F. and Boutekedjiret, C. (2015) Extraction: Steam Distillation. Reference Module in Chemistry, Molecular Sciences and Chemical Engineering. Elsevier, Amsterdam. https://doi.org/10.1016/B978-0-12-409547-2.11557-4

[10] CLSI Clinical and Laboratory Standards Institute (2012) Methods for Dilution Antimicrobial Susceptibility Tests for Bacteria That Grow Aerobically; Approved Standard (9th ed.). 32, 13 p.

[11] Araújo, M.M. and Longo, P.L. (2016) *In Vitro* Antibacterial Activity of *Origanum vulgare* (Oregano) Essential Oil against *Escherichia coli* and *Staphylococcus aureus* Strains. *Arquivos do Instituto Biologico*, **83**, 1-7. https://doi.org/10.1590/1808-1657000702014

[12] Ghabraie, M., Vu, K.D., Tata, L., Salmieri, S. and Lacroix, M. (2016) Antimicrobial Effect of Essential Oils in Combinations against Five Bacteria and Their Effect on Sensorial Quality of Ground Meat. *LWT—Food Science and Technology*, **66**, 332-339. https://doi.org/10.1016/j.lwt.2015.10.055

[13] Paglione, I.S., Galindo, M.V., Medeiros, J.A.S., Yamashita, F., Alvim, I.D., Grosso, C.R.F., Sakanaka, L.S. and Shirai, M.A. (2019) Comparative Study of the Properties of Soy Protein Concentrate Films Containing Free and Encapsulated Oregano Essential Oil. *Food Packaging and Shelf Life*, **22**, Article ID: 100419. https://doi.org/10.1016/j.fpsl.2019.100419

[14] Hunterlab (1997) The Color Management Company. Universal Software, Version 3.2, Reston.

[15] R Core Team (2020) R: A Language and Environment for Statistical Computing. R Foundation for Statistical Computing, Vienna. https://www.R-project.org

[16] RStudio Team (2022) RStudio: Integrated Development for R. RStudio, PBC, Boston. http://www.rstudio.com

[17] Barbosa, I.M., Medeiros, J.A.C., Oliveira, K.A.R., Gomes-Neto, N.J., Tavares, J.F., Magnani, M. and Souza, E.L. (2016) Efficacy of the Combined Application of Oregano and Rosemary Essential Oils for the Control of *Escherichia coli*, *Listeria monocytogenes* and *Salmonella* Enteritidis in Leafy Vegetables. *Food Control*, **59**, 468-477. https://doi.org/10.1016/j.foodcont.2015.06.017

[18] Kosakowska, O., Weglarz, Z., Pióro-Jabrucka, E., Przybyl, J.L., Krasniewska, K., Gniewosz, M. and Baczek, K. (2021) Antioxidant and Antibacterial Activity of Essential Oils and Hydroethanolic Extracts of Greek Oregano (*O. vulgare* L. subsp. hirtum (Link) Ietswaart) and Common Oregano (*O. vulgare* L. subsp. vulgare). *Molecules*, **26**, Article No. 988. https://doi.org/10.3390/molecules26040988

[19] Cariri, M.L., Mello, A.N.F., Mizzi, L., Ritter, A.C., Tondo, E., Souza E.L., Valdramidis, V. and Magnani, M. (2019) Quantitative Assessment of Tolerance Response to Stress after Exposure to Oregano and Rosemary Essential Oils, Carvacrol and 1,8-cineole in *Salmonella* Enteritidis 86 and Its Isogenic Deletion Mutants Δdps, ΔrpoS and ΔompR. *Food Research International*, **122**, 679-687. https://doi.org/10.1016/j.foodres.2019.01.046

[20] Silva, N., Alves, S., Gonçalves, A., Amaral, J.S. and Poeta, P. (2013) Antimicrobial Activity of Essential Oils from Mediterranean Aromatic Plants against Several Foodborne and Spoilage Bacteria. *Food Science and Technology International*, **19**, 503-510. https://doi.org/10.1177/1082013212442198

[21] Alvarez, M.V., Ortega-Ramirez, L.A., Silva-Espinoza, B.A., Gonzalez-Aguilar, G.A.

and Ayala-Zavala, J.F. (2019) Antimicrobial, Antioxidant, and Sensorial Impacts of Oregano and Rosemary Essential Oils over Broccoli Florets. *Journal of Food Processing and Preservation*, **43**, Article 13889. https://doi.org/10.1111/jfpp.13889

[22] Cid-Pérez, T.S., Ávila-Sosa, R., Ochoa-Velasco, C.E., Rivera-Chavira, B.E. and Nevárez-Moorillón, G.V. (2019) Antioxidant and Antimicrobial Activity of Mexican Oregano (*Poliomintha longiflora*) Essential Oil, Hydrosol and Extracts from Waste Solid Residues. *Plants*, **8**, Article No. 22. https://doi.org/10.3390/plants8010022

[23] Chaftar, N., Girardot, M., Labanowski, J., Ghrairi, T., Hani, K., Frere, J. and Imbert, C. (2016) Comparative Evaluation of the Antimicrobial Activity of 19 Essential Oils. In: Donelli, G., Ed., *Advances in Microbiology. Infectious Diseases and Public Health*, Vol. 901, Springer, Berlin, 1-15. https://doi.org/10.1007/5584_2015_5011

[24] Nazzaro, F., Fratianni, F., Martino, L., Coppola, R. and Feo, V. (2013) Effect of Essential Oils on Pathogenic Bacteria. *Pharmaceuticals*, **6**, 1451-1474. https://doi.org/10.3390/ph6121451

[25] Brozyna, M., Paleczny, J., Kozlowska, W., Chodaczek, G., Dudek-Wicher, R., Felinczak, A., Golebiewska, J., Górniak, A. and Jumka, A. (2021) The Antimicrobial and Antibiofilm *in Vitro* Activity of Liquid and Vapour Phases of Selected Essential Oils against *Staphylococcus aureus*. *Pathogens*, **10**, Article No. 1207. https://doi.org/10.3390/pathogens10091207

[26] Burt, S. (2004) Essential Oils: Their Antibacterial Properties and Potential Applications in Foods—A Review. *International Journal of Food Microbiology*, **94**, 223-253. https://doi.org/10.1016/j.ijfoodmicro.2004.03.022

[27] López, P., Sánchez, C., Batlle, R. and Nerín, C. (2005) Solid- and Vapor-Phase Antimicrobial Activities of Six Essential Oils: Susceptibility of Selected Foodborne Bacterial and Fungal Strains. *Journal of Agriculture and Food Chemistry*, **53**, 6939-6946. https://doi.org/10.1021/jf050709v

[28] Fokom, R., Adamou, S., Essono, D., Ngwasiri, D.P., Eke, P., Teugwa Mofor, C., Tchoumbougnang, F., Fekam, B.F., Amvam Zollo, P.H., Nwaga, D. and Sharma, A.K. (2019) Growth, Essential Oil Content, Chemical Composition and Antioxidant Properties of Lemongrass as Affected by Harvest Period and Arbuscular Mycorrhizal Fungi in Field Conditions. *Industrial Crops and Products*, **138**, Article ID: 111477. https://doi.org/10.1016/j.indcrop.2019.111477

[29] Seydim, A.C. and Sarikus, G. (2006) Antimicrobial Activity of Whey Protein Based Edible Films Incorporated with Oregano, Rosemary and Garlic Essential Oils. *Food Research International*, **39**, 639-644. https://doi.org/10.1016/j.foodres.2006.01.013

[30] Liu, Q.R., Wang, W., Qi, J., Huang, Q. and Xiao, J. (2019) Oregano Essential Oil Loaded Soybean Polysaccharide Films: Effect of Pickering Type Immobilization on Physical and Antimicrobial Properties. *Food Hydrocolloids*, **87**, 165-172. https://doi.org/10.1016/j.foodhyd.2018.08.011

[31] Sani, M.A., Ehsani, A. and Hashemi, M. (2017) Whey Protein Isolate/Cellulose Nanofibre/TiO_2 Nanoparticle/Rosemary Essential Oil Nanocomposite Film: Its Effect on Microbial and Sensory Quality of Lamb Meat and Growth of Common Foodborne Pathogenic Bacteria during Refrigeration. *International Journal of Food Microbiology*, **251**, 8-14. https://doi.org/10.1016/j.ijfoodmicro.2017.03.018

[32] Abdollani, M., Rezaei, M. and Farzi, G. (2012) A Novel Active Bionanocomposite Film Incorporating Rosemary Essential Oil and Nanoclay into Chitosan. *Journal of Food Engineering*, **111**, 343-350. https://doi.org/10.1016/j.jfoodeng.2012.02.012

[33] Nedorostova, L., Kloucek, P., Kokoska, K., Stolcova, M. and Pulkrabek, J. (2009)

Antimicrobial Properties of Selected Essential Oils in Vapour Phase against Foodborne Bacteria. *Food Control*, **20**, 157-160. https://doi.org/10.1016/j.foodcont.2008.03.007

[34] Hyun, J.E., Bae, Y.M., Yoon, J.H. and Lee, S.Y. (2015) Preservative Effectiveness of Essential Oils in Vapor Phase Combined with Modified Atmosphere Packaging against Spoilage Bacteria on Fresh Cabbage. *Food Control*, **51**, 307-313. https://doi.org/10.1016/j.foodcont.2014.11.030

[35] Gõni, P., López, P., Sánchez, C., Gómez-Lus, R., Becerril, R. and Nerín, C. (2009) Antimicrobial Activity in the Vapour Phase of a Combination of Cinnamon and Clove Essential Oils. *Food Chemistry*, **116**, 982-989. https://doi.org/10.1016/j.foodchem.2009.03.058

[36] Madigan, M.T., Martinko, J.M. and Bender, K.S. (2016) Microbiologia de Brock. Grupo A, Porto Alegre, 1032 p.

[37] Hyldgaard, M., Mygind, T. and Meyer, R.L. (2013) Essential Oils in Food Preservation: Mode of Action, Synergies, and Interactions with Food Matrix Components. *Frontiers in Microbiology*, **3**, Article No. 12. https://doi.org/10.3389/fmicb.2012.00012

[38] Chen, C., Xu, Z., Ma, Y., Liu, J., Zhang, Q., Tang, Z., Fu, K., Yang, F. and Xie, J. (2018) Properties, Vapour-Phase Antimicrobial and Antioxidant Activities of Active Poly(vinyl alcohol) Packaging Films Incorporated with Clove Oil. *Food Control*, **88**, 105-112. https://doi.org/10.1016/j.foodcont.2017.12.039

[39] Cao, T.L. and Song, K.B. (2019) Effects of Gum Karaya Addition on the Characteristics of Loquat Seed Starch Films Containing Oregano Essential Oil. *Food Hydrocolloids*, **97**, Article ID: 105198. https://doi.org/10.1016/j.foodhyd.2019.105198

[40] Shen, Y., Zhou, J., Yang, C., Chen, Y., Yang, Y., Zhou, C., Wang, L., Xia, G., Yu, X. and Yang, H. (2022) Preparation and Characterization of Oregano Essential Oil-Loaded *Dioscorea zingiberensis* Starch Film with Antioxidant and Antibacterial Activity and Its Application in Chicken Preservation. *International Journal of Biological Macromolecules*, **212**, 20-30. https://doi.org/10.1016/j.ijbiomac.2022.05.114

[41] Saricaoglu, F.T. and Turhan, S. (2020) Physicochemical, Antioxidant and Antimicrobial Properties of Mechanically Deboned Chicken Meat Protein Films Enriched with Various Essential Oils. *Food Packaging and Shelf Life*, **25**, Article ID: 100527. https://doi.org/10.1016/j.fpsl.2020.100527

[42] Xu, J., Liu, F., Wang, T., Goff, H.D. and Zhong, F. (2020) Fabrication of Films with Tailored Properties by Regulating the Swelling of Collagen Fiber through pH Adjustment. *Food Hydrocolloids*, **108**, Article ID: 106016. https://doi.org/10.1016/j.foodhyd.2020.106016

[43] Damodaran, S., Parkin, K.L. and Fennema, O.R. (2010) Química de Alimentos de Fennema. 4th Edition, Artemed, Porto Alegre.

[44] Salgado, P.R., López-Caballero, M.E., Gómez-Guillén, M.C., Mauri, N.A. and Montero, M.P. (2013) Sunflower Protein Films Incorporated with Clove Essential Oil Have Potential Application for the Preservation of Fish Patties. *Food Hydrocolloids*, **33**, 74-84. https://doi.org/10.1016/j.foodhyd.2013.02.008

[45] Know, S.J., Chang, Y. and Han, J. (2017) Oregano Essential Oil-Based Natural Antimicrobial Packaging Film to Inactivate *Salmonella enterica* and Yeasts/Molds in the Atmosphere Surrounding Cherry Tomatoes. *Food Microbiology*, **65**, 114-121. https://doi.org/10.1016/j.fm.2017.02.004

[46] Stani, C., Vaccari, L., Mitri, E. and Birarda, G. (2020) FTIR Investigation of the Secondary Structure of Type I Collagen: New Insight into the Amide III Band.

Spectrochimica Acta Part A: *Molecular and Biomolecular Spectroscopy*, **229**, Article ID: 118006. https://doi.org/10.1016/j.saa.2019.118006

[47] Valderrama, A.C.S. and De, G.C.R. (2017) Traceability of Active Compounds of Essential Oils in Antimicrobial Food Packaging Using a Chemometric Method by ATR-FTIR. *American Journal of Analytical Chemistry*, **8**, 726-741. https://doi.org/10.4236/ajac.2017.811053

[48] Popa, R.M., Fetea, F. and Socaciu, C. (2021) ATR-FTIR-MIR Spectrometry and Pattern Recognition of Bioactive Volatiles in Oily versus Microencapsulated Food Supplements: Authenticity, Quality, and Stability. *Molecules*, **26**, Article No. 4837. https://doi.org/10.3390/molecules26164837

Supplementary Material

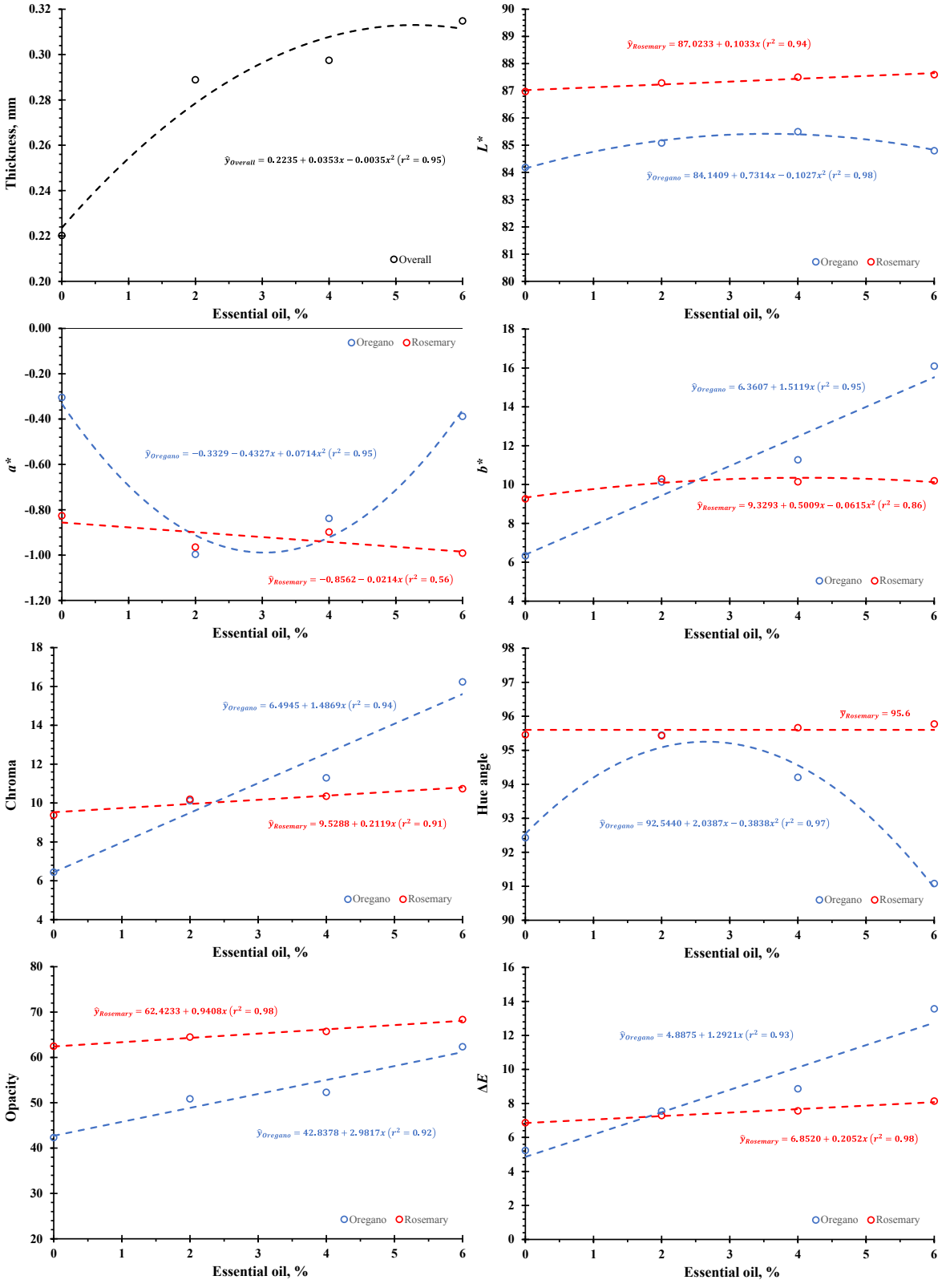

Figure S1. Thickness and color traits from collagen fiber plus polyvinyl alcohol films with oregano (*Origanum vulgare* L.) or rosemary (*Rosmarinus officinalis* L.) essential oil levels.

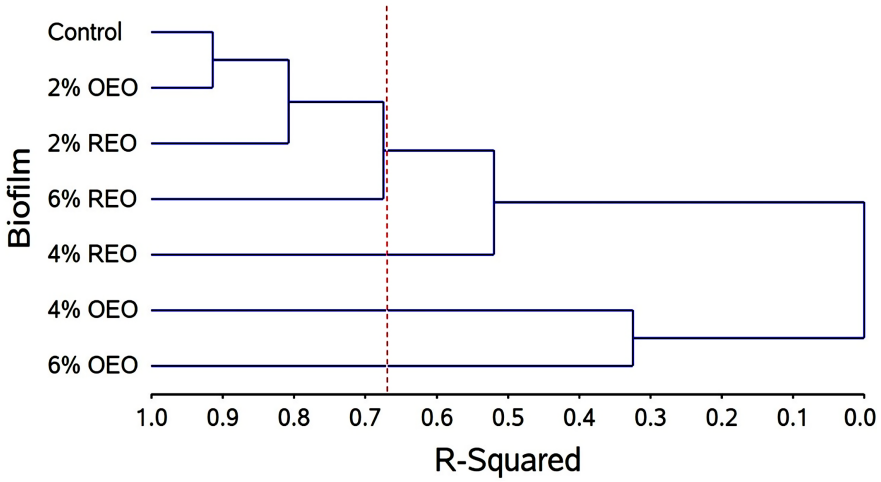

(A)

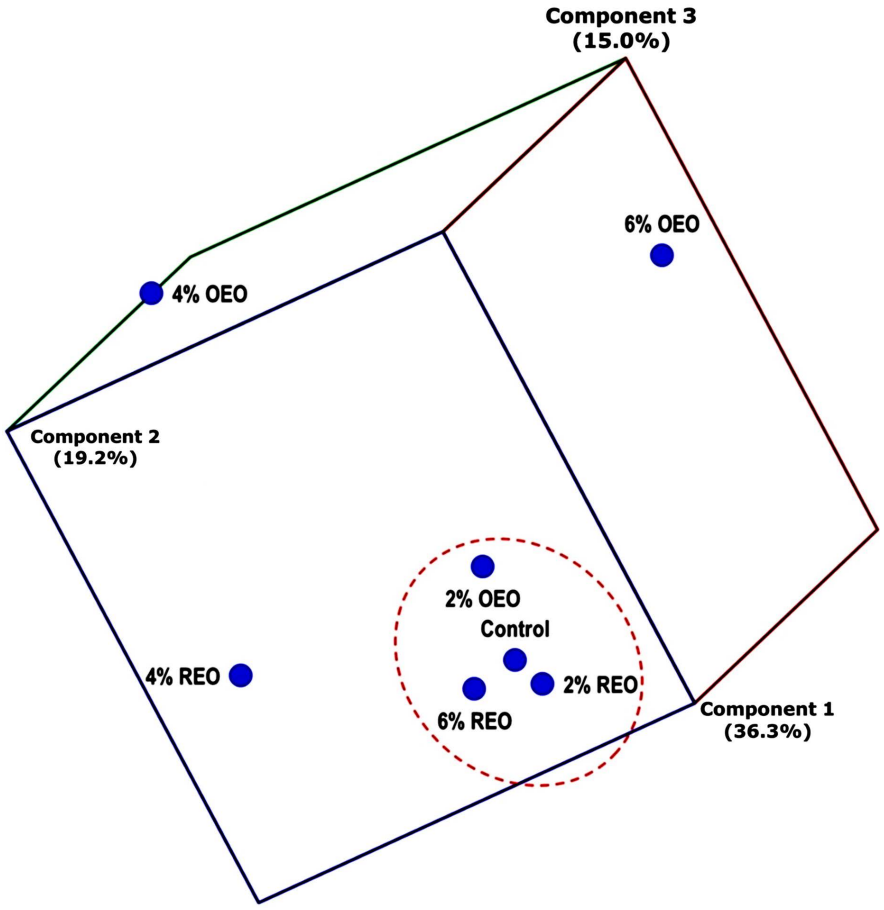

(B)

Figure S2. Dendrogram of Fourier-transform infrared (FTIR) spectrum (4000 to 400 cm^{-1}) data from collagen fiber plus polyvinyl alcohol films without (control) and with oregano (*Origanum vulgare* L. - OEO) or rosemary (*Rosmarinus officinalis* L. - REO) essential oil levels (2%, 4%, and 6%), ordinate axis, in relation to the coefficient of determination (r^2), abscissa axis, using Euclidean distance as dissimilarity measure and Ward's agglomerative hierarchical algorithm as clustering method (A) and three-dimensional graphic dispersion of the treatments in relation to the principal components (B).

Table S1. Probability values of fixed effects and their interactions for disk diffusion and micro-atmosphere from collagen fiber plus polyvinyl alcohol films.

Sources of variation	Dependent variables	
	Disk diffusion	Micro-atmosphere
Essential oil type (T)	0.0001	0.0001
Essencial oil level (L)	0.0001	0.0001
Bacteria (B)	0.0001	0.0001
T × L	0.0001	0.0001
T × B	0.0001	0.0001
L × B	0.0001	0.0001
T × L × B	0.0001	0.0001
Mean	1.72	7.50
Standard error of the mean (SEM)	0.12	0.86
Coefficient of variation (CV)	18.8	5.65
Coefficient of determination (r^2)	0.97	0.99

Table S2. Bacterial susceptibility in disk diffusion (mm) from collagen fiber plus polyvinyl alcohol films with oregano (*Origanum vulgare* L.) or rosemary (*Rosmarinus officinalis* L.) essential oil levels.

Bacteria (B)[1]	Essential oil level (L), %				Mean
	0	2	4	6	
			Oregano		
EC	0.00^{c}	0.02^{Cc}	1.63^{Bb}	6.09^{Ba}	1.93
LMB	0.00^{c}	1.42^{ABb}	1.78^{Bb}	3.22^{Da}	1.61
LMSA	0.00^{d}	0.96^{Bc}	1.85^{Bb}	7.19^{Aa}	2.50
PA	0.00^{c}	1.54^{Ab}	1.58^{Bb}	3.25^{Da}	1.59
SA	0.00^{c}	0.04^{Cc}	1.38^{Bb}	5.08^{Ca}	1.63
ST	0.00^{c}	1.72^{Ab}	2.75^{Aa}	3.11^{Da}	1.89
Mean[2]	0.00	0.95	1.83	4.66	
			Rosemary		
EC	0.00^{c}	2.17^{Ab}	2.49^{Ab}	3.39^{Aa}	2.01
LMB	0.00^{b}	1.85^{ABa}	1.92^{Ba}	2.35^{Ba}	1.53
LMSA	0.00^{c}	1.57^{Bb}	1.84^{Bb}	2.59^{Ba}	1.50
PA	0.00^{c}	1.35^{Bb}	1.79^{Bab}	2.09^{Ba}	1.31
SA	0.00^{b}	2.21^{Aa}	2.42^{Aa}	2.63^{Ba}	1.82

Continued

ST	0.00[c]	1.48[Bb]	1.79[Bb]	2.42[Ba]	1.42
Mean[3]	0.00	1.77	2.04	2.58	

Means followed by different capital letters within the same column and different small letters within the same row differ ($p < 0.05$), respectively, between bacteria and essential oil levels by the Student Newman Keuls test. [1]EC = *Escherichia coli*; LMB = *Listeria monocytogenes* (Biofilm); LMSA = *Listeria monocytogenes* (Scott A); PA = *Pseudomonas aeruginosa*; SA = *Staphylococcus aureus*; ST = *Salmonella typhimurium*.

[2] $\hat{y}_{Oregano} = -0.3877 + 0.7511x\left(r^2 = 0.90\right)$. [3] $\hat{y}_{Rosemary} = 0.3962 + 0.4002x\left(r^2 = 0.86\right)$.

Table S3. Bacterial susceptibility in micro-atmosphere (mm) from collagen fiber plus polyvinyl alcohol films with oregano (*Origanum vulgare* L.) or rosemary (*Rosmarinus officinalis* L.) essential oil levels.

Bacteria (B)[1]	Essential oil level (L), %				Mean
	0	2	4	6	
			Oregano		
EC	0.00[c]	0.00[c]	17.7[Ab]	36.7[Aa]	13.6
LMB	0.00[b]	0.00[b]	0.00[Cb]	26.9[Ba]	6.72
LMSA	0.00[b]	0.00[b]	0.00[Cb]	25.5[Ca]	6.38
PA	0.00[b]	0.00[b]	0.00[Cb]	24.0[Da]	5.99
SA	0.00[c]	0.00[c]	15.3[Bb]	37.0[Aa]	13.1
ST	0.00[b]	0.00[b]	0.00[Cb]	27.1[Ba]	6.77
Mean[2]	0.00	0.00	5.50	29.5	
			Rosemary		
EC	0.00[c]	0.00[c]	21.4[Ab]	25.1[Aa]	11.6
LMB	0.00[b]	0.00[b]	0.00[Bb]	15.1[Da]	3.78
LMSA	0.00[b]	0.00[b]	0.00[Bb]	19.4[Ca]	4.84
PA	0.00[b]	0.00[b]	0.00[Bb]	19.0[Ca]	4.74
SA	0.00[c]	0.00[c]	21.0[Ab]	25.2[Aa]	11.6
ST	0.00[b]	0.00[b]	0.00[Bb]	24.3[Ba]	6.06
Mean[3]	0.00	0.00	7.06	21.3	

Means followed by different capital letters within the same column and different small letters within the same row differ ($p < 0.05$), respectively, between bacteria and essential oil levels by the Student Newman Keuls test. [1]EC = *Escherichia coli*; LMB = *Listeria monocytogenes* (Biofilm); LMSA = *Listeria monocytogenes* (Scott A); PA = *Pseudomonas aeruginosa*; SA = *Staphylococcus aureus*; ST = *Salmonella typhimurium*.

[2] $\hat{y}_{Oregano} = 0.7737 - 4.6594x + 1.5560x^2\left(r^2 = 0.98\right)$.

[3] $\hat{y}_{Rosemary} = -0.0014 - 1.7599x + 0.8813x^2\left(r^2 = 0.99\right)$.

Table S4. Results of univariate analysis of variance (ANOVA) for thickness and color traits from collagen fiber plus polyvinyl alcohol films.

Variables	Sources of variation[1]			Mean	Contrast (L)[2]		
	T	L	T × L		C × W	Linear	Quadratic
Thickness	0.1304	0.0001	0.3652	0.278	0.0001	0.0001	0.0035
L^*	0.0001	0.0001	0.0242	86.2	0.0001	0.0001	0.0002
a^*	0.0001	0.0001	0.0001	−0.78	0.0001	0.0037	0.0001
b^*	0.0001	0.0001	0.0001	10.3	0.0001	0.0001	0.9601
Chroma	0.0001	0.0001	0.0001	10.3	0.0001	0.0001	0.1103
Hue angle	0.0001	0.0001	0.0001	94.4	0.0001	0.0002	0.0001
Opacity	0.0001	0.0001	0.0001	59.1	0.0001	0.0001	0.0075
ΔE	0.0001	0.0001	0.0001	8.03	0.0001	0.0001	0.0001

[1]T = essential oil type (Oregano or Rosemary); L = essential oil level (0%, 2%, 4%, or 6%); T × L = type and level interaction. [2]C × W = control (0%) × with essential oil (2%, 4% e 6%); and a linear or quadratic tendency for essential oil level (L).